


Radiolabeling and Preliminary Evaluation of ^{99m}Tc -Labeled DNA Cube Nanoparticles as Potential Tracers for SPECT Imaging

Xiaoyan Duan¹Yiri Du¹Chunmei Wang^{1,2}Zhenfeng Zhao^{1,2}Chao Li¹Jianbo Li^{1,2} 

¹Inner Mongolia Medical University Affiliated Hospital, Hohhot, 010050, People's Republic of China; ²Inner Mongolia Key Laboratory of Molecular Imaging, Hohhot, 010050, People's Republic of China

Purpose: DNA nanostructures, with the advantages of structural designability and spatial addressability, have shown a great potential in the field of drug delivery and bio-medicine. Herein, we aimed to prepare technetium-99m radiolabeled DNA cube nanoparticles (^{99m}Tc -DCN) and expect to build a DCN-based drug carrier and nuclear medicine imaging platform.

Methods: DCN could be readily assembled with 6 designed DNA oligonucleotides at an equal mole ratio in a single annealing procedure. ^{99m}Tc -MAG3-ssDNA (A20) was obtained by labeling MAG3-ssDNA (A20) with technetium-99m by using a stannous chloride reduction method. ^{99m}Tc -DCN was prepared by hybridize DCN with side chains (T20-DCN) with ^{99m}Tc -MAG3-ssDNA (A20). The biodistribution study and SPECT/CT imaging were conducted on KM mice.

Results: DCN was successfully assembled, and as-prepared DCN was characterized by native polyacrylamide gel electrophoresis, atomic force microscope and fluorescence resonance energy transfer. The size of DCN was about 5 nm. The radiolabeling yield of ^{99m}Tc -MAG3-ssDNA (A20) was approximately 90% by radio thin-layer chromatography. T20-DCN mixed with ^{99m}Tc -MAG3-ssDNA (A20) in PBS could generate ^{99m}Tc -DCN upon hybridization. The retention time (RT) of ^{99m}Tc -MAG3-ssDNA (A20) was at ~22 min, and the RT of as-prepared ^{99m}Tc -DCN was at ~12 min by radio-HPLC. The results from biodistribution study and SPECT/CT imaging showed that a significant proportion of DCNs were metabolized through the liver and kidney. Intestine exhibited a relatively indicative signal as well, which might be explained by the enterohepatic circulation of DCN via the liver and gallbladder.

Conclusion: We have successfully prepared ^{99m}Tc -DCN as a SPECT/CT imaging probe via the side-chain hybridization strategy. The probe was metabolized mainly by the liver and excreted primarily to the bladder. Due to the superior properties of DNA cube nanoparticles, we believe DCN may potentially be translated into a preclinical setting for diagnosis and treatment of cancer-related diseases.

Keywords: DNA cube nanoparticles, Tc-99m labeling, biodistribution, SPECT/CT imaging

Introduction

Nuclear medicine imaging is to introduce a small amount of imaging drugs called “probes” into the body and use emission computed tomography equipment to explore the dynamic and/or static distribution of “probes” in the human body or target organs. These probes have the same or similar physiological and biochemical characteristics as the natural metabolites in the human body, so as to understand the changes in the functions, physiology and biochemistry, metabolism and gene expression of human organs. Single photon emission computed tomography

Correspondence: Jianbo Li
Inner Mongolia Medical University
Affiliated Hospital, No. 1 Tongdao North
Street, Hohhot, 010050, People's Republic
of China
Tel/Fax +86 471 345 1574
Email lijianbo_1235@msn.cn

(SPECT), one of the molecular imaging methods in nuclear medicine, involves the use of radioisotope-labelling probes. It has the advantages over other imaging modalities (such as optical imaging, computed tomography, magnetic resonance imaging, etc.) in high sensitivity, deep penetration depth, and the possibility to perform functional imaging.^{1,2} Extensive efforts have been made in SPECT imaging to collect more detailed in-vivo information by using different radioisotope-labelling probes.^{3–5} Nanotechnologies in the development of smart molecular imaging platforms are supplying potential imaging probes for multimodal imaging, which combine the advantages of various imaging modalities in order to improve specificity and sensitivity to the target.^{6–8}

DNA nanotechnology is a technology for artificially designing DNA strand sequences, following the base-pairing rules to combine DNA strands into a double helix structure, finally forming a defined and robust three-dimensional structure. This technology can be used to predict and design complex DNA nanostructures. In this field, DNAs are used as non-biological nanomaterials, rather than as genetic information carriers for living cells. DNA nanostructures, which can be functionalized with different targeting ligands (such as organic molecules, peptides, antibody, aptamer and so on),⁹ display excellent delivery capacity for various drugs (such as CpG, doxorubicin, or siRNA), as well as signal moieties (fluorescent dyes or radionuclides). These signal molecules can be utilized to explore the in-vivo information of DNA nanostructures including biodistribution, metabolism and stability properties. DNA nanostructures, with the advantages of structural designability and spatial addressability, have shown a great potential in the field of biosensing,^{10–12} drug delivery,^{13–15} and bio-medicine.^{16–19}

DNA cube nanoparticles (DCN),²⁰ a classic example of DNA nanostructures, could be readily assembled with 6 designed DNA oligonucleotides. To successfully prepare DCN, we designed a set of six short oligonucleotides for self-assembly, and the results supported our establishment of DCN. MAG3 was chosen for Tc-99m chelation since we preferred a smaller and more hydrophilic ligand for radiolabeling. Herein, we aimed to prepare technetium-99m radiolabeled DCN (^{99m}Tc-DCN), apply the as-formed ^{99m}Tc-DCN for SPECT imaging to investigate its in-vivo biodistribution properties and pharmacokinetics profiles, and expect to build a DCN-based drug carrier and nuclear medicine imaging platform.

Materials and Methods

General

Sodium Pertechnetate [^{99m}Tc] was supplied by HTA Co., Ltd. (Beijing, China), with radionuclide purity (⁹⁹Mo% <5*10⁻²%) and radiochemical purity (>98%). Tris(hydroxymethyl)aminomethane (Tris base, ≥99.8%) was purchased from Merck Limited (Beijing, China). All other analytical reagents were purchased from Sinopharm Chemical Reagent Co., Ltd. (SCRC, Shanghai, China) and used as received unless stated otherwise.

The interested tissues and organs from the biodistribution study were measured with a γ -counter (SN-697, Shanghai Rihuan Photoelectronic Instrument Co., Ltd.). NanoScan SPECT/CT (Mediso Ltd., Hungary) was used to conduct SPECT/CT imaging.

Preparation of DNA Cube Nanoparticles

DCNs were prepared via a single annealing procedure^{20,21} similar to the method which was used to prepare DNA bipyramid nanostructures (DBNs).³ In brief, equal molar quantities (1 μ M) of six single-strand DNA (a, b, c, d, e, and f) with designated sequences, which were purchased from TaKaRa Biotechnology Co., Ltd. (Dalian, China), were mixed in TM buffer (10 mM Tris base and 50 mM MgCl₂, pH 8.0), heated to 95°C for 10 min, and then cooled to 4°C for 20 min. The oligonucleotide sequences of each single-strand DNA (ssDNA) used in the study are listed in Table 1.

PAGE Characterization of DCN

The single-step annealing process of DCN was analyzed using native polyacrylamide gel electrophoresis (PAGE). The as-formed DNA samples were run in 8% PAGE gel in TAE-Mg buffer at 4°C for about 2 h. The gel was stained with GelRed DNA gel stain solution (Biotium, Inc., Hayward, CA, USA) for 15 min and analyzed by the chemiluminescence imaging system (G:Box Chemi-XL, Syngene, A Division of Synoptics Ltd., Cambridge, United Kingdom). The yields of DCNs were semi-quantitatively determined by using ImageJ analysis software (NIH, Bethesda, MD, USA).

FRET for Verifying Correct Assembly of DCN

Fluorescence resonance energy transfer (FRET) technique was used to detect the correct assembly of DCN. Cy3 and Cy5 were chosen as FRET donors and

Table 1 The Oligonucleotide Sequences of Each ssDNA Used in the Study

ssDNA	Sequence
a	GGCAACTTTGATCCCTCAGGTTTAGCGCCGGTCCTTTCTCCCACTACTTTCACTG
b	GGGAAACTTTCGTGTGTAGGTTTTGTTGCCAGTGTTTCTACGATGTACTTTGGTC
c	GGACATTTTCGAGATCAGCATTTGTTTCCCGACCTTTGCGTGATTGTATTTAGAG
d	GGCGCTTTTGACACTTCTGCTTTATGTCCCTCTATTTCTTAGATGACTTTTGACC
e	GGGAGATTAGTCATCTAAGTTTACAATCACGCTTTGTACATCGTAGTTTGTAGT
f	GGGATCTTTACCTACACACGTTTGTCTGATCTCGTTTGCAGAAGTGCTTTCTCTGA
a-T20	TTTTTTTTTTTTTTTTTTTTGGCAACTTTGATCCCTCAGGTTTAGCGCCGGTCCTTTCTCCCACTACTTTCACTG
A20	AAAAAAAAAAAAAAAAAAAA
Cy3-b	Cy3-GGGAAACTTTCGTGTGTAGGTTTTGTTGCCAGTGTTTCTACGATGTACTTTGGTC
Cy5-c	GGACATTTTC(Cy5)GAGATCAGCATTTGTTTCCCGACCTTTGCGTGATTGTATTTAGAG

acceptors, respectively. FRET-DCN was assembled with another set of six ssDNA (a, Cy3-b, Cy5-c, d, e and f). Oligonucleotide sequences of Cy3-b and Cy5-c are listed in Table 1. Cy3-b and Cy5-c were obtained by connecting Cy3 with b strand at 5' end and connecting Cy5 with c strand at the tenth base from 5' end. FRET-DCN was excited using the 535 nm laser line, and the fluorescent signal was measured using a fluorescence spectrophotometer (Hitachi F-4500 Fluorescence Spectrophotometer).

HPLC for Purifying DCN

DCNs were purified by high performance liquid chromatography (HPLC, Agilent 1100 chromatography system, Agilent Technologies) with a size exclusive chromatography column (Phenomenex® BioSec-SEC-4000, 300*7.8 mm). The mobile phase is 150 mM NaCl with a flow rate of 0.3 mL/min. The solution was concentrated with 30 kDa Amicon Ultra-0.5 mL centrifugal filters (EMD Millipore Corporation) at 3000 g for 20 min. The concentration of purified DCN was measured by their absorbance at 260 nm with a UV spectrophotometer (HITACHI U-3010).

Atomic Force Microscope Imaging of DCN

DCN (2 µL, 20 nM) was deposited onto a freshly cleaved mica cell and left to adsorb for 2–3 min. 1×TAE-Mg²⁺ buffer (400 µL) was added to the liquid cell, and the sample was scanned in a tapping mode

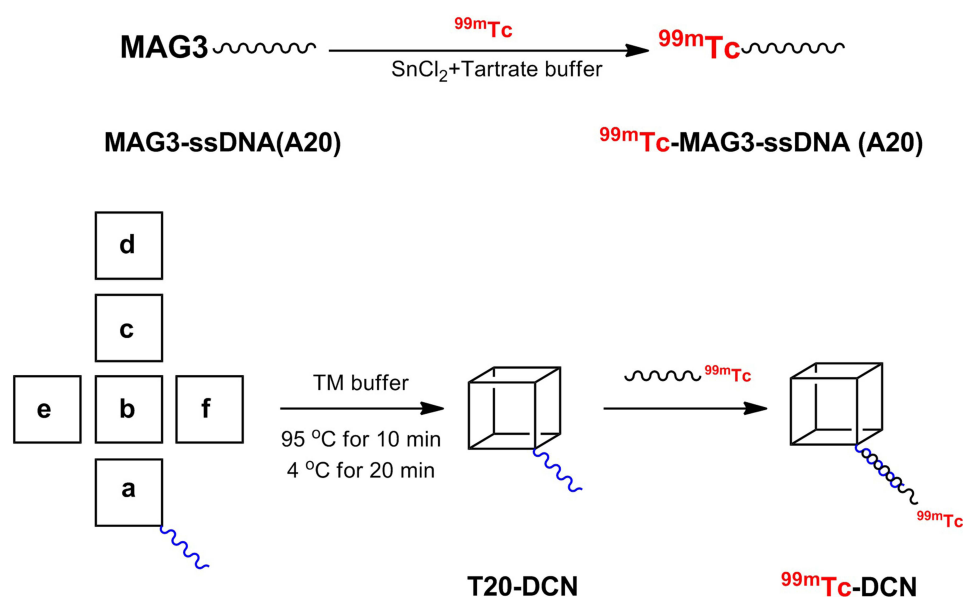
under fluid on a Pico-Plus AFM (Agilent Technologies, Santa Clara, CA, USA) with NP-S tips (Veeco, Inc., Oyster Bay, NY, USA).

Preparation of MAG3-ssDNA (A20)

The experimental procedure of MAG3-ssDNA (A20) preparation followed the study published previously in our lab.³ In brief, 300 µg NHS-MAG3 ester and 250 µg ssDNA (A20) were mixed gently in 0.3 M HEPES (100 µmol/L, pH 8.0) at room temperature and incubated for 2 h. The reaction was terminated by adding 50 µL ammonium acetate (2 mol/L) to the mixture. MAG3-ssDNA (A20) was purified through a NAP-5 column (GE) with 0.25 mol/L ammonium acetate as eluent.

Radiolabeling of DCN

First, ^{99m}Tc-MAG3-ssDNA (A20) was obtained by labeling MAG3-ssDNA (A20) with technetium-99m by using a stannous chloride reduction method. MAG3-ssDNA (A20) was mixed with 10 µL tartrate buffer (50 mg/mL), 5 µL SnCl₂ solution (4 mg/mL, freshly prepared), and finally 25 µL sodium pertechnetate [^{99m}Tc] (~10 mCi) for 20 min at 95°C. Then, when the temperature of the reaction solution dropped to room temperature, DCN with side chains (T20-DCN) was added into the reaction solution to hybridize with ^{99m}Tc-MAG3-ssDNA (A20), which was showed in Scheme 1. Last, ^{99m}Tc-DCN were analyzed and purified through Radio-HPLC system.



Scheme 1 Schematic display of the assembly and radiolabeling process of ^{99m}Tc -DCN.

In-vivo Biodistribution Study

The biodistribution study of DCN was conducted by injecting 200 μL ^{99m}Tc -DCN ($\sim 10 \mu\text{Ci}$) into KM mice via tail vein. The mice ($n=5$ at each time point) were sacrificed by cervical dislocation and dissected, and interested tissues or organs were collected to measure radioactivity by a γ -counter at 60 sec counting periods. Uptake values were corrected for radio-decay and expressed as the percentage of injected dose per gram of tissue (%ID/g).

Small Animal SPECT/CT Imaging

In SPECT/CT imaging, ^{99m}Tc -DCN ($\sim 500 \mu\text{Ci}$ for each mouse) was injected into KM mice ($n=5$) via the tail vein without anesthesia. After 1 h post injection, the mice were anesthetized by inhaling the isoflurane (1.5%)-oxygen mixture, and placed prone on the scanning bed for SPECT/CT imaging by nanoScan SPECT/CT with large FOV (12 cm X 10 cm). CT scanning was performed following each SPECT acquisition. SPECT and CT images were reconstructed using the MEDISO software and then merged and analyzed using the InVivoScope software (Bioscan).

Results

Preparation and Characterization of DCN

DCN was assembled by six oligonucleotides with designated sequences (a, b, c, d, e, and f) mixed at an equal

mole ratio of about $1 \mu\text{M}$. The as-prepared DCN was characterized by PAGE. With each single-strand oligonucleotide added to the reaction solution, the migration of as-prepared DNA samples would gradually slow down until the final formation of DCN, which is shown in Figure 1A. The size of DCN measured with AFM was about 5 nm (Figure 1B). DCN was assembled correctly, which was proved by FRET. The peak at 665 nm, which is Cy5 emission peak, appeared obviously, while there was almost no peak at 565 nm, which is Cy3 emission peak (Figure 1C). The crude product was purified by HPLC, and the retention time (RT) of DCN was about 14 min (Figure 1D).

Radiolabeling of MAG3-ssDNA

First, S-acetyl-MAG3-NHS was conjugated with NH_2 -ssDNA A(20), and the product MAG3-ssDNA A(20) was radiolabeled by technetium-99m with a single reduction reaction to obtain ^{99m}Tc -MAG3-ssDNA (A20). The yield of the radiolabeling reaction was approximately 90%, and the specific activity (SA) of ^{99m}Tc -MAG3-ssDNA (A20) was 1.0–1.2 mCi/nmol. Radio thin-layer chromatography (Radio-TLC) was used to analyze the radiolabeling yield. Three components would occur during the radiolabeling process: free technetium-99m, technetium hydrogel, and radiolabeled ssDNA. Two developing system was applied during radio-TLC analysis. When developed in 100% acetone, radiolabeled ssDNA and technetium hydrogel would both stay at the original point, while free

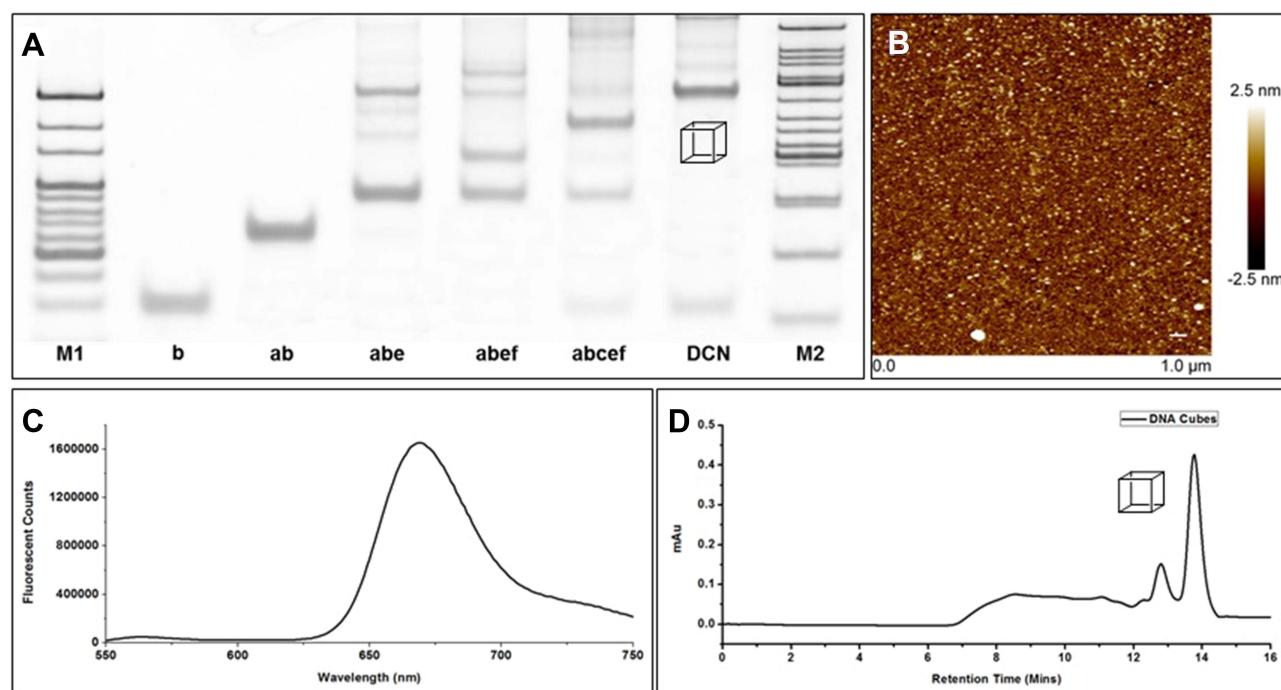


Figure 1 Preparation and Characterization of DCN. (A) Characterization of the DCN self-assembly process by PAGE. M1, 50 bp marker. M2, 20 bp marker; (B) AFM image of DCN. Scale bar: 50 nm; (C) FRET analysis of DCN. A FRET pair (Cy3 and Cy5) was designed on the same vertex of DCN, and FRET effect could be observed during the assembly of DCN; (D) HPLC analysis of DCN, and the retention time was about 14 min.

technetium would move to the solvent front. Moreover, when developed by saline (0.9% sodium chloride), only technetium hydrogel would stay at the original spot, while radiolabeled ssDNA and free technetium would migrate to the solvent front. Then, by a simple subtraction, we could calculate the radiochemistry purity of radiolabeled ssDNA. As shown in Figure 2, almost no free technetium was observed, and technetium hydrogel was about 8% in the reaction solvent. Thus, the radiochemistry purity of ^{99m}Tc -MAG3-ssDNA (A20) prepared was about 92%.

Radiolabeling of DCN

In Scheme 1, a sequence of T(20) was designed to the 5' end of oligonucleotide a, and the as-formed DCN thus had a T(20) side chain (T20-DCN), which made it available for hybridization with an A(20) single-stranded DNA (ssDNA). Radiolabeling of DCN could be readily achieved by hybridization between ^{99m}Tc -MAG3-ssDNA (A20) and T20-DCN. T20-DCN mixed with ^{99m}Tc -MAG3-ssDNA (A20) in phosphate saline buffer (PBS, pH 7.4) under mild shaking conditions at room temperature for 5–10 min could generate ^{99m}Tc -DCN upon hybridization, and the estimated SA of radiolabeled DCN was in the range of 6.0–7.2 mCi/nmol. Radio-HPLC was used for analysis and

purification of radiolabeled DCN for in vivo investigation. As shown in Figure 3, the RT of ^{99m}Tc -MAG3-ssDNA (A20) was at ~22 min, and the RT of as-prepared ^{99m}Tc -DCN was at ~12 min, indicative of the successful preparation of radiolabeled DCN (^{99m}Tc -DCN).

In-vivo Biodistribution Study

We investigated the biodistribution pattern of ^{99m}Tc -DCN in healthy mice, denoted as the percent injected dose per

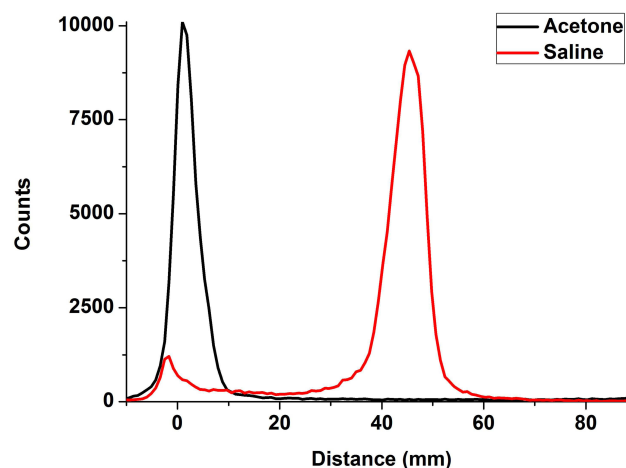


Figure 2 Radio-TLC image of ^{99m}Tc -MAG3-ssDNA (A20) under 2 developing system. Black line: 100% Acetone; Red line: 0.9% saline.

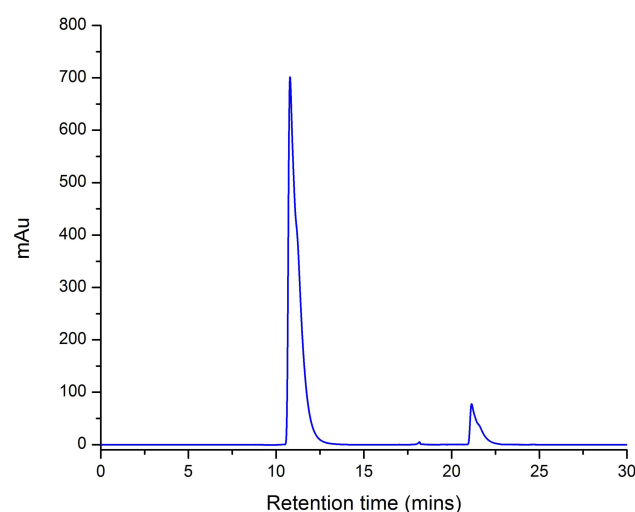


Figure 3 Radio-HPLC analysis of DNA samples. The RT of ^{99m}Tc -DCN was at ~12 min, and ^{99m}Tc -MAG3-ssDNA (A20) was at ~22 min.

gram organ (%ID/g). As shown in Figures 4, ^{99m}Tc -DCN in the blood pool peaked at 5 min after injection, and then rapidly decreased later on, suggesting a rapid distribution of DCN in vivo. Within 4 hours after injection, the tracer uptake in the heart, lung, intestine, stomach and brain was never higher than 5%ID/g, while accumulation in the liver dropped from about $16.33 \pm 1.86\%$ ID/g at 15 min to around $0.18 \pm 2.29\%$ ID/g at 4 h after injection. In the kidneys, ^{99m}Tc -DCN had reached about $27.84 \pm 1.66\%$ ID/g at 5 min after injection, and then decreased rapidly to about $7.62 \pm 0.26\%$ ID/g and $0.59 \pm 0.08\%$ ID/g at 60 min and 4 h after injection, respectively. As for the tracer uptake in the spleen, ^{99m}Tc -DCN dropped down from $4.25 \pm 0.76\%$ ID/g at 5 min to $0.59 \pm 0.27\%$ ID/g at 4 h after injection.

Small Animal SPECT/CT Imaging

Finally, SPECT/CT imaging of ^{99m}Tc -DCN in healthy mice was performed, and metabolic pathway of DCN in vivo was analysed. As shown in Figure 5, after intravenous injection of ^{99m}Tc -DCN for 1 h, a significant amount of ^{99m}Tc -DCN was seen in the bladder. Moreover, the gallbladder and intestine showed a high uptake of ^{99m}Tc -DCN.

Discussion

The innovation of nanotechnology has made considerable progress in the field of biomedical research, including drug delivery, targeted therapy, molecular imaging, and biosensing. Among them, DNA nanotechnology uses natural or artificial DNA strands as constituent elements to prepare 2D and 3D nanostructures through specific interactions between DNA molecules, namely Watson–Crick base pairing. DNA nanostructures have the advantages of easy construction, controllable structure and size/shape, as well as multiple chemical modification pathways, and exhibit unprecedented versatility in terms of complexity and programmability, which provides a versatile platform for biomedical applications. The oligonucleotide strands constituting DNA nanostructures can be covalently linked with small molecules, proteins or nucleic acid, endowing DNA nanostructures with a stable structure under physiological conditions, high targeting and affinity, high cellular uptake rate, or improved delivery capacity of molecular cargo, etc., which enhanced the function of DNA nanostructures in biological environments. DCN, which is assembled with 6 designed DNA oligonucleotides, is one of DNA nanostructures, and possesses the characteristics

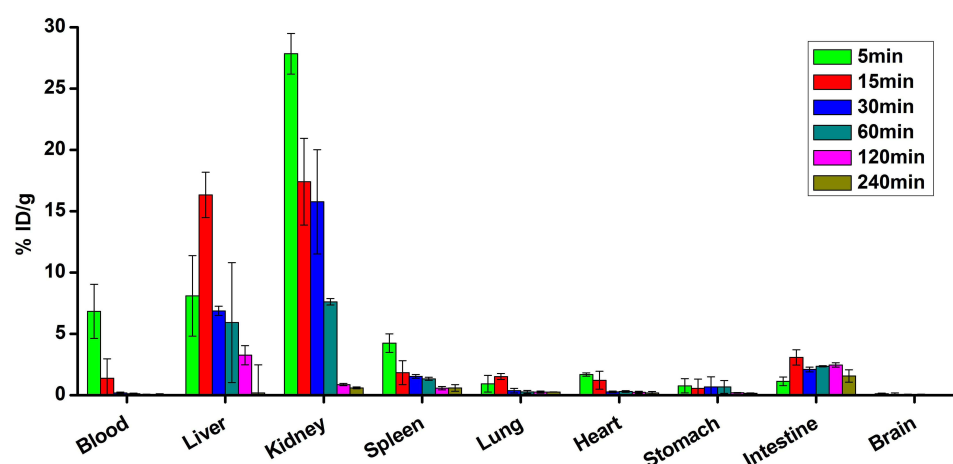


Figure 4 Biodistribution profile (%injected dose per gram organ, %ID/g organ) of ^{99m}Tc -DCN in healthy mice.

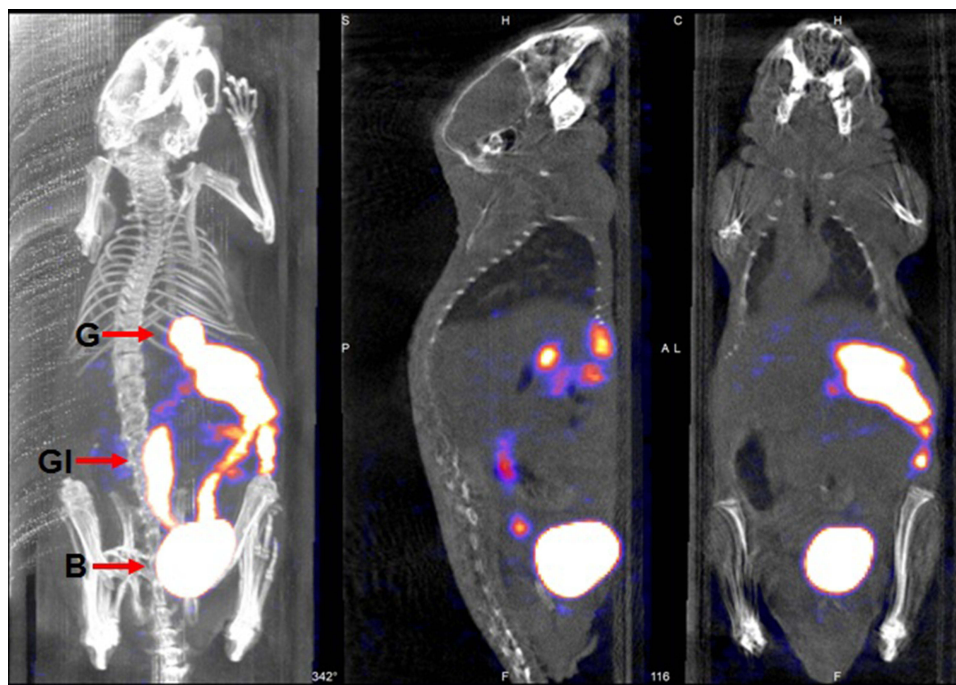


Figure 5 SPECT/CT images of ^{99m}Tc -DCN in a healthy mouse at 1 h p.i. Middle: sagittal position; Right, coronal position.
Abbreviations: B, bladder; G, gallbladder; GI, GI Tract.

of DNA nanostructure described above. We would like to further understand the feasibility of DCN as molecular imaging probes in this study.

DCN was successfully assembled by six oligonucleotides with designated sequences via a single annealing procedure. The as-prepared DCN was characterized by PAGE and FRET, purified by HPLC, and further used for technetium-99m labeling experiment. Technetium-99m labeled DCN was prepared by side-arm chain hybridization, which is consistent with the preparation method of technetium-99m labeled DNA bipyramid reported in the literature.³ MAG3-ssDNA (A20) was labeled with technetium-99m to obtain ^{99m}Tc -MAG3-ssDNA (A20) using a stannous chloride reduction method. ^{99m}Tc -MAG3-ssDNA (A20) was hybridized with DCN with side chains (T20-DCN) to prepare ^{99m}Tc -DCN.

Intravenous injection of ^{99m}Tc -DCN was done to reveal its biodistribution in healthy mice, and the half-life of ^{99m}Tc -DCN was calculated to be around 5 min, which was similar to the reported blood half-life of technetium-99m labeled DBNs³ and was about two-fold longer than the blood half-life of double-stranded DNA (dsDNA) reported previously.⁶ DNA analogs, in the form of single-stranded antisense oligonucleotides or aptamers, have been radiolabeled for cancer imaging. However, these tracers showed extremely fast blood clearance in vivo, with an

estimated circulation half-life of 2–3 min. Limited by this rapid excretion, DNA analogs-based imaging probes presented limited tumor accumulation. Also, single-stranded or double-stranded oligonucleotides have poor serum stability. Studies have found that after folding into 3D nanostructures (such as tetrahedron, bipyramid, or cubes), their serum stability improved significantly. The prolonged circulation of ^{99m}Tc -DCN in vivo suggested different biological properties of DCN, indicating an intrinsic physiological property of folded 3D nanostructures in vivo. By measuring the accumulation of ^{99m}Tc -DCN in organs of interest, we defined the specific biodistribution pattern of DCN in vivo, which showed an efficient renal excretion (from $27.84 \pm 1.66\%$ ID/g at 5 min after injection to $0.59 \pm 0.08\%$ ID/g at 4 h after injection) and an elongated retention than common dsDNA reported previously,⁶ yet displayed some similarity with other nanoparticles with diameters less than 5 nm (such as quantum dots²²) in mice. As for DBNs, the uptake of tracer in the liver remained at a high level (above 20% ID/g) until 2 hours after injection. In the kidney, spleen and small intestine, the distribution trend of the two imaging agents (^{99m}Tc -DCN and ^{99m}Tc -DBNs) was similar.³

The results of SPECT/CT imaging were consistent with the results of biodistribution experiment, that the gallbladder showed a high uptake of ^{99m}Tc -DCN, suggesting that a

significant proportion of DCN was indeed metabolized within the liver. However, in SPECT/CT imaging, the intestine exhibited a relatively indicative signal either, which might be explained by the enterohepatic circulation of DCN via the liver and gallbladder.

Conclusion

In conclusion, we have successfully radiolabeled DNA cube nanoparticles with a gamma-ray emission isotope (Technetium-99m) and prepared ^{99m}Tc -DCN as a SPECT/CT imaging probe via a side-chain hybridization strategy. The biodistribution pattern of the probe has been investigated, and SPECT/CT imaging of ^{99m}Tc -DCN was performed for preliminary evaluation. The probe was metabolized mainly by the liver and excreted primarily to the bladder. The relatively short half-life of this probe would minimize the radiation dose to ease the concern of radiation hazard, and the excellent biodegradability of DCN would cause minimal toxicity to animals. Due to the superior properties of DNA cube nanoparticles, we believe DCN may potentially be translated into a preclinical setting for diagnosis and treatment of cancer-related diseases.

Abbreviations

AFM, atomic force microscope; DBNs, DNA bipyramid nanostructures; DCN, DNA cube nanoparticles; FRET, fluorescence resonance energy transfer; HPLC, high performance liquid chromatography; PAGE, polyacrylamide gel electrophoresis; PET, positron emission computed tomography; Radio-TLC, radio thin-layer chromatography; RT, retention time; SsDNA, single-strand DNA; SPECT, single photon emission computed tomography.

Data Sharing Statement

All data generated or analysed during this study are included in this published article.

Ethics Approval and Consent to Participate

The animal study protocol had been approved by the Medical Ethics Committee of Inner Mongolia Medical University. The animal experiments were performed in accordance with the 'Guide for the Care and Use of Laboratory Animals' (Institute of Laboratory Animal Resources, Commission on Life Sciences, National

Research Council, ISBN: 0-309-58869-3, 140 pages, 1996).

Acknowledgments

The abstract of this paper was presented at the SNMMI 2018 Annual Meeting as a poster presentation with interim findings. The poster's abstract was published in "Poster Abstracts" in Journal of Nuclear Medicine: https://jnm.snmjournals.org/content/59/supplement_1/1069.

Funding

National Natural Science Foundation of China (No. 82060324), Natural Science Foundation of Inner Mongolia (2018LH08044) and Science and Technology Program of Inner Mongolia (2019GG106).

Disclosure

The authors declare that they have no conflicts of interest for this work.

References

1. Massoud TF, Gambhir SS. Molecular imaging in living subjects: seeing fundamental biological processes in a new light. *Gene Dev.* 2003;17(5):545–580. doi:10.1101/gad.1047403
2. Saji H. In vivo molecular imaging. *Biol Pharm Bull.* 2017;40(10):1605–1615. doi:10.1248/bpb.b17-00505
3. Li J, Jiang D, Bao B, He Y, Liu L, Wang X. Radiolabeling of DNA bipyramid and preliminary biological evaluation in mice. *Bioconjugate Chem.* 2016;27(4):905–910. doi:10.1021/acs.bioconjchem.5b00680
4. Zhao L, Shi X, Zhao J. Dendrimer-based contrast agents for PET imaging. *Drug Deliv.* 2017;24(S1):81–93. doi:10.1080/10717544.2017.1399299
5. Jiang Y, Gai Y, Long Y, et al. Application and evaluation of [^{99m}Tc]-labeled peptide nucleic acid targeting MicroRNA-155 in breast cancer imaging. *Mol Imaging.* 2020;19:1536012120916124. doi:10.1177/1536012120916124
6. Jiang D, Sun Y, Li J, et al. Multiple-armed tetrahedral DNA nanostructures for tumor-targeting, dual-modality in vivo imaging. *ACS Appl Mater Inter.* 2016;8(7):4378–4384. doi:10.1021/acsami.5b10792
7. Gao P, Wei R, Liu X, et al. Covalent organic framework-engineered polydopamine nanoplateform for multimodal imaging-guided tumor photothermal-chemotherapy. *Chem Commun.* 2021;57(46):5646–5649. doi:10.1039/D1CC00314C
8. Tejwan N, Saini AK, Sharma A, Singh TA, Kumar N, Das J. Metal-doped and hybrid carbon dots: a comprehensive review on their synthesis and biomedical applications. *J Control Release.* 2021;330:132–150. doi:10.1016/j.jconrel.2020.12.023
9. Henry SJW, Stephanopoulos N. Functionalizing DNA nanostructures for therapeutic applications. *WIREs Nanomed Nanobio.* 2021;e1729. doi:10.1002/wnan.1729
10. Zhao D, Kong Y, Zhao S, Xing H. Engineering functional DNA–protein conjugates for biosensing, biomedical, and nanoassembly applications. *Topics Curr Chem.* 2020;378(3):41. doi:10.1007/s41061-020-00305-7

11. Zhao X, Ma R, Hu Y, et al. Translocation of tetrahedral DNA nanostructures through a solid-state nanopore. *Nanoscale*. 2019;11(13):6263–6269. doi:10.1039/C8NR10474C
12. Li C, Hu X, Lu J, et al. Design of DNA nanostructure-based interfacial probes for the electrochemical detection of nucleic acids directly in whole blood. *Chem Sci*. 2018;9(4):979–984. doi:10.1039/C7SC04663D
13. Wu T, Liu Q, Cao Y, et al. Bundle DNA tetrahedron for efficient regulation of gene expression. *ACS Appl Mater Inter*. 2020;12(29):32461–32467. doi:10.1021/acsami.0c08886
14. Tian T, Zhang T, Zhou T, Lin S, Shi S, Lin Y. Synthesis of an ethyleneimine/tetrahedral DNA nanostructure complex and its potential application as a multi-functional delivery vehicle. *Nanoscale*. 2017;9(46):18402–18412. doi:10.1039/C7NR07130B
15. Jiang D, England CG, Cai W. DNA nanomaterials for preclinical imaging and drug delivery. *J Control Release*. 2016;239(2016):27–38. doi:10.1016/j.jconrel.2016.08.013
16. Chen Q, Ding F, Zhang S, et al. Sequential therapy of acute kidney injury with a DNA nanodevice. *Nano Lett*. 2021;21(10):4394–4402. doi:10.1021/acs.nanolett.1c01044
17. Duangrat R, Udomprasert A, Kangsamaksin T. Tetrahedral DNA nanostructures as drug delivery and bioimaging platforms in cancer therapy. *Cancer Sci*. 2020;111(9):3164–3173. doi:10.1111/cas.14548
18. Jiang D, Ge Z, Im H-J, et al. DNA origami nanostructures can exhibit preferential renal uptake and alleviate acute kidney injury. *Nat Biomed Eng*. 2018;2(11):865–877. doi:10.1038/s41551-018-0317-8
19. Xie X, Shao X, Ma W, et al. Overcoming drug-resistant lung cancer by paclitaxel loaded tetrahedral DNA nanostructures. *Nanoscale*. 2018;10(12):5457–5465. doi:10.1039/C7NR09692E
20. Chen J, Seeman NC. Synthesis from DNA of a molecule with the connectivity of a cube. *Nature*. 1991;350(6319):631–633. doi:10.1038/350631a0
21. Edwardson TGW, Carneiro KMM, McLaughlin CK, Serpell CJ, Sleiman HF. Site-specific positioning of dendritic alkyl chains on DNA cages enables their geometry-dependent self-assembly. *Nat Chem*. 2013;5(10):868–875. doi:10.1038/nchem.1745
22. Nguyen KC, Zhang Y, Todd J, et al. Biodistribution and systemic effects in mice following intravenous administration of cadmium telluride quantum dot nanoparticles. *Chem Res Toxicol*. 2019;32(8):1491–1503. doi:10.1021/acs.chemrestox.8b00397

International Journal of Nanomedicine

Dovepress

Publish your work in this journal

The International Journal of Nanomedicine is an international, peer-reviewed journal focusing on the application of nanotechnology in diagnostics, therapeutics, and drug delivery systems throughout the biomedical field. This journal is indexed on PubMed Central, MedLine, CAS, SciSearch®, Current Contents®/Clinical Medicine,

Journal Citation Reports/Science Edition, EMBase, Scopus and the Elsevier Bibliographic databases. The manuscript management system is completely online and includes a very quick and fair peer-review system, which is all easy to use. Visit <http://www.dovepress.com/testimonials.php> to read real quotes from published authors.

Submit your manuscript here: <https://www.dovepress.com/international-journal-of-nanomedicine-journal>